Journal of Material Cycles and Waste Management (2022) 24:2229–2242
https://doi.org/10.1007/s10163-022-01470-1

ORIGINAL ARTICLE

New method for producing carbon foam from recycled carbon (NEWCAFO)

Senay Balbay[1,2,3] · **Caglayan Acıkgoz**[4]

Received: 25 October 2021 / Accepted: 19 July 2022 / Published online: 16 August 2022

Abstract

The aim of the study was to define a new method (SENAY process) for carbon foam (CF) production following curing by mixing organic materials with high-volatile content only with acrylic resins. In the study, carbon foam was produced by calcining after curing in water-based acrylic resins (styrene acrylic copolymer (SAC) and vinyl acrylic copolymer (VAC)) and recycled carbon (RC) obtained from decomposed waste tire. The amount of RC (3–5 g), SAC:VAC ratio (5:0–0:5), temperature (400–900 °C), and time (30–240 min) were selected as parameters. Carbon foams were characterized by porosity tests and FT-IR (Fourier transform infrared spectrophotometer), SEM (scanning electron microscope), TEM (transmission electron microscope), and BET (Brunauer–Emmett–Teller) analysis. The porosity values of CF-1: 1, CF-1: 3, and CF-0: 5 carbon foams were 75.71, 79, and 97%, respectively. Porosity value was 97% due to the micropores and nanoparticles seen in the bonds of CF-0:5 where only VAC was used. As a result, a simple and cost-effective new method for carbon foam production has been verified as a result of curing by mixing organic materials with high-volatile matter content and only acrylic resins without using pressure and stabilization steps. At the same time, a new area where waste tire can be utilized in the production of carbon foam has been demonstrated.

Graphical abstract

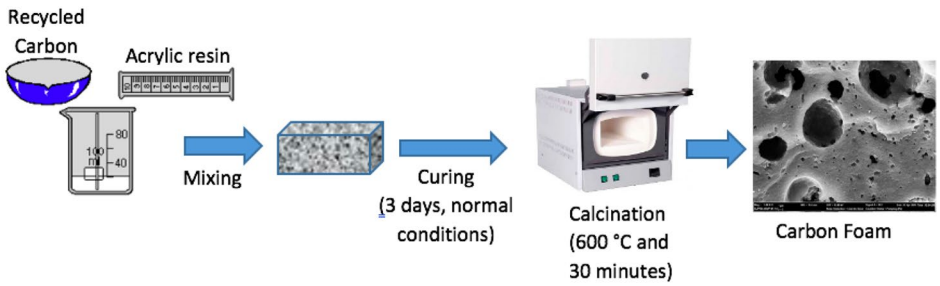

A new method for produced of carbon foams is at 600 °C in 30 minutes using acrylic resins and recycled carbon.

Keywords Carbon foam · Waste tire · Acrylic resin · Recycling · Circular economy

✉ Senay Balbay
senay.balbay@bilecik.edu.tr

[1] Vocational School, Department of Environmental Protection Technologies, Bilecik Seyh Edebali University, Bilecik 11230, Turkey

[2] Central Research Laboratory Application and Research Center, Bilecik Seyh Edebali University, Bilecik 11230, Turkey

[3] Graduate School Institute, Industrial Sustainability Department, Bilecik Seyh Edebali University, Bilecik 11230, Turkey

[4] Faculty of Engineering, Department of Chemistry Engineering, Bilecik Seyh Edebali University, Bilecik 11230, Turkey

Introduction

Each year, 1.5 billion tons in the world [1, 2], 4.5 million tons in the USA [3], approximately, 3.6 million tons in Europe [4] and 300,000 tons in Turkey [5] of End-of-Life Tire (ELT) are emerging. Only 15–20% of the ELTs in the world are used again and 75–80% of it spills on the earth [1]. 80% of waste tires in Turkey and the world cannot be used and waste tires that are abandoned, i.e., thrown into the nature, continue to increase approximately twice every year. Therefore, it is of great importance that waste tires are degraded and used as raw materials [5, 6]. Disposal of waste polymers is a major environmental problem for both municipalities and governments, as polymeric materials do not decompose easily. The direct discharge of waste tires to the environment poses a serious problem for the environment and human health, especially with the chemical spills spread to the receiving environment and because it creates a risk of fire [7, 8]. Therefore, the direct discharge of waste tires to the environment is prohibited by laws and regulations. People and/or facilities that cause waste tire-based environmental pollution have to pay the expenses to compensate for the related damage. Various global and national policies developed around the world are designed for the disposal of solid wastes such as plastic and waste tires [3–5, 9–11]. Many methods for the recycling of waste tire have been given in the literature. Among these methods, material recovery was carried out by pyrolysis [12–16], chemical degradation [17, 18], and devulcanization [19] methods [17]. In the 2015/13034 patent, the waste tire was inflated in concentrated H_2SO_4 at a temperature of 140 °C and 20 min, and then a carbon-based material was obtained by mixing with a mixture of CH_3OH and NaOH [17, 18]. The main obstacles to the practical applications of carbon foam production are that it is produced with complex processes and high cost. This material has been successfully used in the fields of rubber composite material production [20], glass fiber reinforced epoxy composite material production [21, 22], and organic dye adsorption [23]. When the properties of this material were examined, it was determined that it could be used as a carbon source for carbon foam production, and no study was found in which waste tire was used for carbon foam production.

Carbon foams are new generation macroporous carbon materials due to their properties such as cell structure, lightness, high thermal stability, high thermal and electrical conductivity, low density, high porosity, high-pressure strength, fire resistance, excellent electromagnetic and sound absorption and has attracted great attention in many high technology applications in recent years [24–26].

Carbon foam with 93% porosity was produced by performing freeze-drying and carbonization (30 min, 1000 °C) processes using polyvinyl pyrrolidone (PVP) and starch as the carbon source [26]. Carbon foam with 90.06% porosity was synthesized as a result of the carbonization at 1000 °C for 2 h of lignin–resorcinol–glyoxal (LRG) resin as a carbon source and polyurethane (PU) foam as a sacrificial template [27]. As a result of the carbonization of the melamine sponge at 800 °C for 3 h, a double-layered and hierarchically porous carbon foam was obtained [28]. Carbon foam was produced by pyrolyzing commercial melamine foam in a tube furnace for 2 h at 800 °C under N_2 atmosphere [29]. Carbon foam with 80–95% porosity was obtained from polyisocyanurate foam in a tube furnace at 600–700 °C for 1 h [30]. Carbon foam was produced from a mixture of borax, $NaHCO_3$ and wheat flour by carbonizing at 400 °C for the first 2 h and then at 900 °C for 2 h [31]. Carbon foam was prepared from sawdust and sucrose solution by filter pressing at 2 h 900 °C [24]. Carbon foam was produced at 2 h 800 °C using urea, sodium hydroxide, and cotton [32]. As a result of the carbonization (900 °C for 30 min) of steel wool, table sugar, and urea foam, carbon foam with less porosity was obtained [33]. Ultra-black carbon aerogel foam was produced from resorcinol–formaldehyde aerogel of carbon aerogel nanoparticles grown on carbonized melamine foam and melamine foam skeletons as a result of pre-freezing technology and high-temperature calcination [34]. In the PU foaming process, activated carbon foam was produced by reacting with high activity polyol, toluene diisocyanate, and water of the activated carbon absorbing the waste gas [35]. By mixing Zn powder and sucrose in a ratio of 3:1 by mass, it was heated in the high-pressure reactor at 550 °C for 10 h at a heating rate of 5 °C/min. Then, it was etched with nitric acid solution and washed with distilled water and dried. Thus, a three-dimensional interconnected hollow carbon foam electrode material with nitrogen was obtained [36]. Polymer (raw material source is wide) was washed as dipping to mixing of cellulose solution and metal salt (one or a combination of nickel salt, iron salt, aluminum salt, copper salt, cobalt salt, manganese salt, rubidium salt, and vanadium salt) solutions, and dried. Then, carbonized carbon foam was obtained [37]. A method of preparing a flexible and self-supporting SnS/carbon foam composite is described. First, by dissolving $SnCl_2.2H_2O$ and thioacetamide in a glycol solvent, second, washing the melamine sponge with deionized water and drying, third, impregnating the dried melamine sponge sheet with mixed glycol solution, fourth, washing with anhydrous ethanol, then drying and annealing, SnS/carbon foam was obtained [36].

Recently, due to the growing interest in using naturally renewable materials, as well as the demand for environmental protection and sustainable development, various renewable materials such as bacterial cellulose, banana peel, watermelon, lignin, grapefruit peel, pulp, fish skin, sucrose,

tannins, lignins, and olive seeds, have been used in the preparation of amorphous carbon foams [24, 27, 38].

Traditionally, carbon foams are prepared by foaming bitumen-based or organic polymer resins followed by hardening in an inert atmosphere and carbonization/graphitization [24]. Carbon foam is produced in its most general form by: (i) carbonization of polymer stimulants, (ii) reduction and freeze-drying of carbon-based materials such as graphene oxide or carbon nanotube (CNT), (iii) exfoliating graphite and then compressing it into a foam structure, and (iv) swelling of stimulants such as polyaromatic hydrocarbons following carbonization [39]. The most common of these methods is the method in which polymer stimulants are directly carbonized. Phenolic resin is one of the most popular polymer stimulants due to its high carbonization capacity [27]. Since bitumen-derived carbon foams tend to show a regular graphitic structure, they exhibit better mechanical strength and thermal insulation performance due to their high thermal and electrical conductivity. In contrast, carbon foams prepared from synthetic polymer resins such as phenol–formaldehyde, poly(arylacetylene), polyimides and polybenzoxazine exhibit low thermal and electrical conductivity due to their amorphous structure [24].

Carbon foams have a wide range of applications in the fields of thermal protection, filters, electrodes, catalyst supports, lightweight fire-resistant structures, high-temperature thermal insulation, heat exchangers, heat sink, electromagnetic interference (EMI) protection, acoustic absorption and battery electrodes, catalyst carrier, supercapacitor, lithium-ion batteries, and thermal energy storage tank, thermal conductivity enhancer, various electrochemical measurement electrodes, adsorption and desorption of gas types, cleaning and recovery of oil spills and other contaminants, and reflection of electromagnetic waves [24, 26]. Very good results have been obtained in removing oils and organic solvents from water [27]. Because of their three-dimensional networks, shapes, sizes, cell parameters, carbon structures, and adaptive thermal conductivity, carbon foams are high-quality carbon products used as thermal management materials [40]. Due to their ultralight weight, high specific surface area, the high electronic conductivity, and exceptional resistance to harsh environments, they have shown great potential in the absorption of excess electromagnetic waves (EEW) [38]. Since the liquid hydrogen fuel in rockets must be protected from air friction and all heat factors caused by the sun, thermal insulating carbon-based materials with excellent thermal insulation properties are required for aviation applications [40].

The main obstacles to the practical applications of carbon foam production are that it is produced with complex processes and high cost. Therefore, simplified process and reduced cost are required for the preparation of the carbon foam [26]. In the study, it was aimed to produce carbon foam at a certain temperature (600 °C) and time (30 min) by curing the recycled carbon (RC) obtained from decomposed waste tire in water-based acrylic resins. The study will contribute to the literature by defining a simple and cost-effective new method for carbon foam production using high-volatile organic biomass and acrylic resin. Another contribution of this study to the literature is the production of carbon foam using waste tire as a carbon source.

Materials and methods

Materials

The samples of waste tire scraps (WTS) with a diameter of approximately 4.0 mm and a length of 1.02 cm used in the experiments were provided from a tire retreading facility operating in Denizli. SAC and VAC commercial water-based resins were supplied from Asal Boya Kimya firm. The chemicals of 99% CH_3OH, solid NaOH, 37% HCl, 96% H_2SO_4, and solid NaCl used in experimental studies were purchased from Tekkim.

Methods

Carbon foam was produced as a result of the application of chemical degradation, activation and calcination processes to WTS, respectively (Fig. 1).

Chemical degradation

The chemical degradation process of WTS has been applied according to Patent no: 2015/13034. WTS were swelled in concentrated H_2SO_4 at a rate of 12.27 mL H_2SO_4/g WTS at a temperature of 140 °C and for 20 min. A mixture of CH_3OH–NaOH was prepared in a separate place as solvent in the ratio of 0.05 g NaOH/mL CH_3OH. The WTS swollen in H_2SO_4 and the CH_3OH–NaOH solution were mixed in 15 min at room condition and thus the WTS were degraded. After the degradation process of the waste tires was completed, the mixture formed was filtered, and the solid (waste tire slurry) and liquid phases were separated [17, 18].

Activation

The waste tire slurry was washed 3 times with distilled water. Not to lose the volatile substances in its structure, it was dried at 40 °C during 14 h. After the dried material was

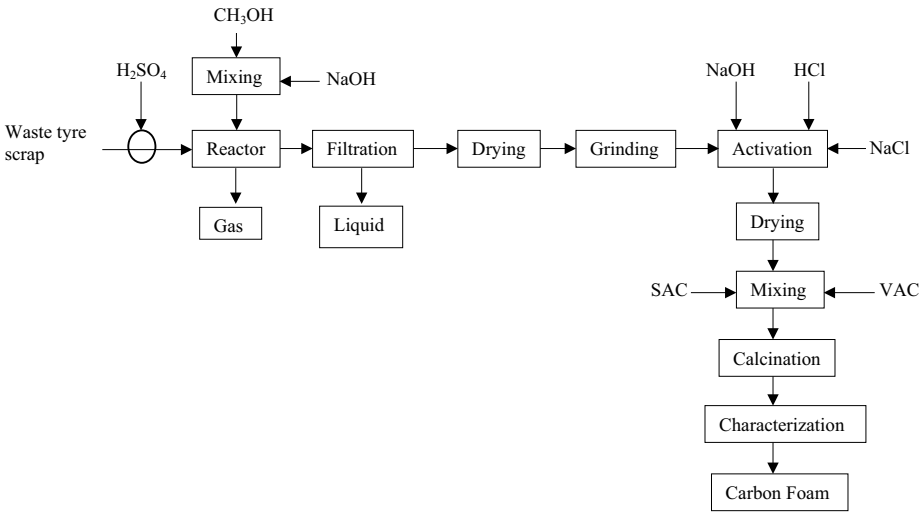

Fig. 1 Carbon foam production flow chart

ground, it was activated with 1 M NaOH, 1 M HCl, and 20% NaCl and dried again to obtain RC [16].

Carbon foam production using SENAY process

After SAC and VAC resins were mixed, RC was added, and after curing for 3 days under normal conditions, carbon foam was produced by applying the calcination process. The most suitable conditions SAC:VAC ratio and RC amount were determined by performing the porosity test according to ASTM (American Society for Testing and Materials) B 962-15 on the produced carbon foams. First, the most suitable RC amount (3–4–5 g) was determined. Second, the calcination temperature (400–500–600–700–800–900 °C) was studied. Third, the optimum calcination time (30–60–120–180–240 min) was fixed. Finally, SAC:VAC ratio (5:0–3:1–1:1–1:3–0:5) was studied. Each experiment was repeated three times. Coding of carbon foams was made according to the parameter studied in each process (eg: CF-3 for 3 g RC study and CF-400 for 400 °C study).

This method, which was defined for the first time in the literature, is called the SENAY process. This method is an easy method that can be used especially for the production of materials from waste. Description of SENAY: **SE**(wa*S*t *E*)**N**(calci*N*atio*N*)**AY**(*A*cr*Y*lic).

Physical and mechanical tests

The porosity tests of the carbon foams obtained were made according to ASTM B 962-15. Carbon foam samples were first boiled in pure water for 40 min to remove the gas in its structure and then cooled. Second, these samples were immersed in water to fill their pores and their weights were determined (A1). Third, the samples were cleaned and weighed (A2). Finally, the samples were dried in the oven for 1 h and weighed (A3). Porosity (%) was calculated according to the following equation:

$$\text{Porosity}(\%) = \frac{A2 - A3}{A2 - A1} \times 100 \quad (1)$$

The density of the carbon foams was measured by the ratio of the mass of the carbon foam to the total volume of the carbon foam. The volumetric shrinkage of carbon foams is the percentage ratio of the volume of carbon foam before calcination to the volume of carbon foam after calcination. The mechanical strengths of carbon foams were determined using the ELE CBR-Test-50.

Characterization

Carbon foams were characterized by surface morphology (SEM-ZEISS Supra 40VP brand scanning electron microscope and JEOL JEM 1220 brand transmission electron microscope), and surface area (Micromeritics ASAP 2020 gas adsorption porosimeter) analysis. The samples were placed on a conductive carbon band and images were obtained using a scanning electron microscopy at 15 kV. A Fourier transform infrared spectrophotometer (Perkin Elmer Spectrum 100 model FT-IR spectrometer) was used at a wavelength range of 400–4000 cm^{-1} to define the functional groups of carbon foams.

Table 1 Elemental and proximate analysis values of WTS and RC [17]

	Fixed car. (%)	VM (%)	Ash (%)	Moisture (%)	C (%)	H (%)	N (%)	O[a] (%)	S (%)	GHV[b] (Mj/kg)
WTS	28.31	64.75	6.94	0	84.77	8.07	1.88	3.96	1.32	38.20
RC	46	41.88	6.91	5.21	67.71	6	0.065	21.35	4.87	27.77

[a]Calculated from the weight difference, [b]calculated by Beckman's formula {GHV (MJ/kg) = 0.352C + 0.944H + 0.105 (S–O)}, *VM* volatile matter

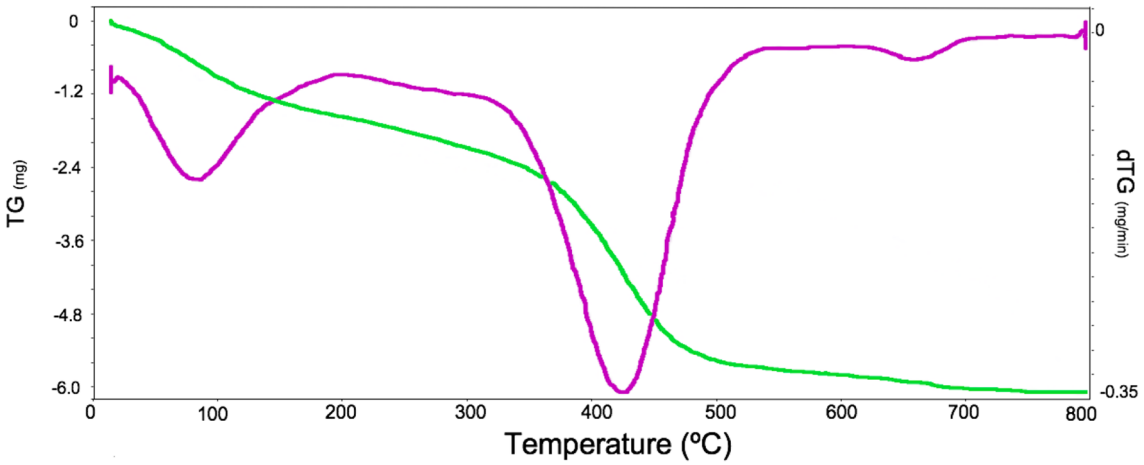

Fig. 2 Thermogravimetry (TG)/differential thermal analysis (DTG) curve of RC [17]

Results and discussion

Carbon foam is a remarkable material with unique properties due to its structure and surface properties and can be produced in different ways [33]. It can usually be synthesized from the polymer (e.g., resin, PU, sucrose, and melamine) directly through a carbonization process [41]. In the study, after curing the mixture of RC and acrylic resin, carbon foam production process was defined as a result of calcination process.

The proximate and elemental analysis results of the RC obtained as a result of chemical degradation and activation of the waste tire are given in Table 1.

It was observed that RC degraded in three stages according to thermogravimetric analysis (TGA) analysis: (i) it degraded by 10% by losing the water in its structure between 30 and 140 °C; (ii) due to the release of some of the volatile components at 140–380 °C, 15% of the RC was degraded; (iii) 25% of RC was degraded due to the release of remaining volatile components at 380–500 °C, and 50% of the RC was degraded between 20 and 520 ºC (Fig. 2) [17].

Carbon foam production

Carbon foams can be produced as a result of the combination of existing a polymer binder and carbon powders such as graphite, graphene and carbon nanotubes [42]. It has high porosity, 3D dimensional and well-bonded honeycomb cell (honeycomb) structure [27, 43, 44]. The most important properties of porous carbons are their large surface area and hierarchical porosity. It is divided into three classes as macropores, mesopores and micropores [45]. In lithium battery studies, it was determined that the main parameter affecting the discharge capacity was mesopore volume [46]. The foam density and other properties of carbon foams determine the porosity and structure of the carbon matrix [47]. Since the porosity parameter in carbon foams was an important parameter in different sectors, the most suitable conditions were determined according to the porosity tests of the carbon foams obtained by studying different RC amounts, different calcination temperatures and times, and different SAC:VAC ratios. Porosity tests were carried out according to ASTM B 962-15 to determine the ratio of the porous volume of the material to its total volume.

One of the foaming methods in carbon foam production is foaming carbon foams using carbon source releasing moisture and volatile substances. During heating, moisture and volatile substances from thermally separated or light fractions are discharged from the carbon source, which makes the carbon foam structure porous and acts as a blowing agent. This type of foaming is called internal foaming or self-bubble [47]. It was cured for 3 days under normal conditions by mixing different amounts of RC (3–4–5 g) at

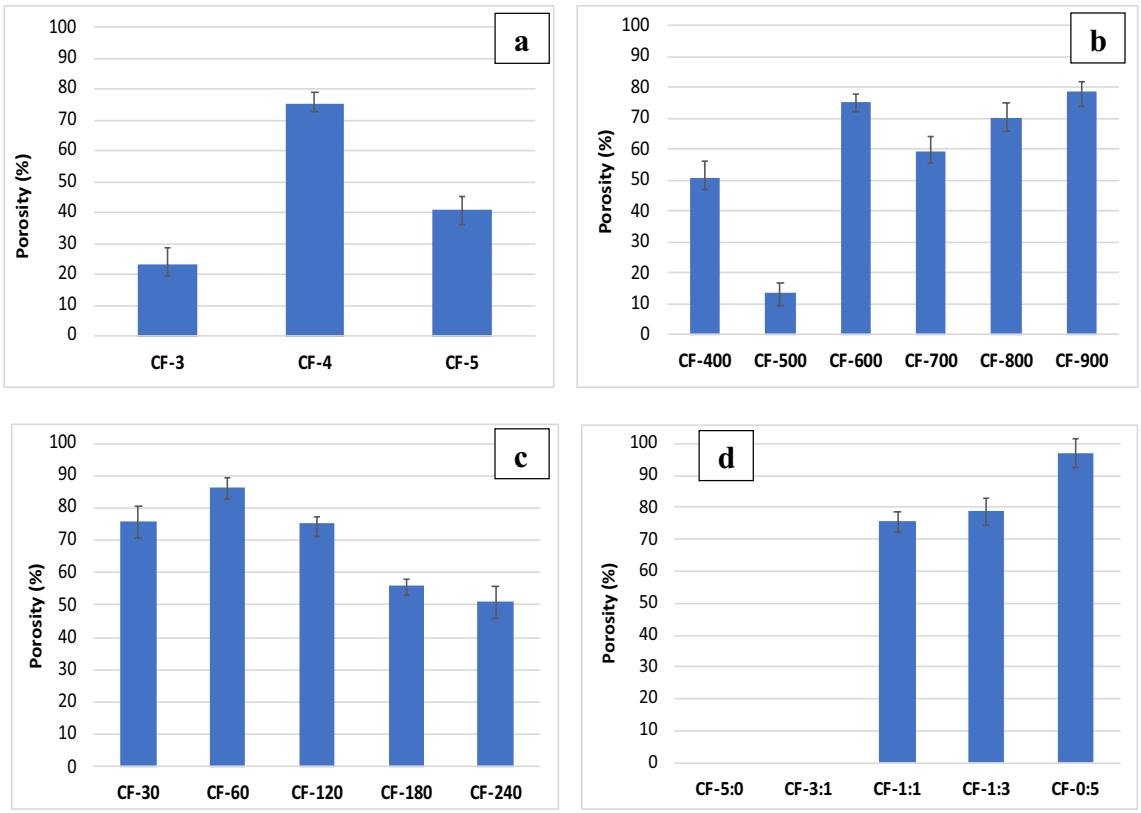

Fig. 3 Porosity values of the carbon foams obtained (a: RC amount, b: temperature, c: time, d: SAC:VAC ratio)

Fig. 4 Photo image of the obtained carbon foam

the ratio of 1:1 SAC:VAC. Calcined at 600 °C for 2 h and according to porosity tests, the most suitable RC amount was determined as 4 g (Fig. 3a). Carbon foam was produced in this new method without using any catalysts or blowing agents due to the effect of volatile matter (41.88%), moisture (5.21%) and oxygen (21.35%) (Table 1) contained in RC. The porosity value was 23.4% with less foam formation due to the insufficient amount of RC in the carbon foam produced using 3 g RC. Due to the high amount of RC in the carbon foam produced using 5 g RC, volatile components

in the carbon foam structure could not be released, so the porosity value was determined as 40.9%. The photographic image of the obtained carbon foam is given in Fig. 4.

With increasing temperature, volatile components were originally developed from thermal breakdown and evaporation of light fractions. Further heating leads to the gradual solidification of the mixture and the fixation of the carbon foam matrix [25]. Under normal conditions, 4 g RC and 1:1 SAC:VAC were cured for 3 days by mixing. It was calcined at different temperatures (400–500–600–700–800–900 °C) in 2 h and the optimum operating temperature was determined as 600 °C according to porosity tests (Fig. 3b). As seen in the TG/DTG curve of RC, the lowest porosity value (13.8%) was observed at 500 °C since all the volatile components in the RC's structure at 380–520 °C reach maximum fluidity (Fig. 2). Starting from 600 °C, depending on the increase in temperature, the carbon matrix was fixed. Porosity values at 600 and 900 °C were 75.36 and 79%, respectively. Since the porosity values for both temperatures were approximately the same, studies were continued at 600 °C to consume less energy.

Under normal conditions, 4 g RC and 1:1 SAC:VAC were mixed and cured for 3 days. The most suitable calcination time was determined according to porosity tests (Fig. 3c) by calcining at 600 °C at different calcination times (30–60–120–180–240 min). The porosity value of the carbon foam obtained at the end of 60 min was the highest, but it was observed that cracks occurred on the sample under the influence of small impacts. For this reason, it was determined that the most suitable working time was 30 min.

Under normal conditions, 4 g of RC and, in different ratios (5:0–3:1–1:1–1:3–0:5), SAC:VAC were cured for 3 days by mixing. The most suitable SAC:VAC ratios were determined according to porosity tests (Fig. 3d) by calcining at 600 °C and in 30 min. It was observed that the samples obtained at the ratios of 5:0 and 3:1 SAC:VAC were dispersed by cracking. Characterization of the CF-1:1, CF-1:3 and CF-0:5 was carried out. The standard deviation values of porosity tests of carbon foams were determined as ≤5% (Fig. 3).

Characterization of carbon foams

Carbon foams were produced as a result of solution polymerization and polycondensation reactions, respectively.

1) Solution polymerization:
   A solvent, monomer and initiator are present in solution polymerization. The solvent chosen for the polymerization reaction should be able to dissolve both the monomer and the polymer formed thoroughly. As the monomer dissolves in the solvent, its concentration decreases over time, so the molecular weight of the polymer obtained increases. Oxygen acts as an inhibitor in many free radicals and solution polymerization [48]. After mixing RC and acrylic resins (Fig. 5), they were cured by solution polymerization in air.
2) Polycondensation reactions:

During the synthesis of carbon foams, polycondensation reactions prevail due to the catalytic effect of sulfur. This helps in the emergence of more aromatic structures, regulation and formation of microcrystalline structures. More extensive polycondensation processes lead to the release of water molecules, resulting in a reduction of the oxygen content in the reaction mixture and helps to form larger crystallites. The release of volatile products and an increase in the amount of oxygen-containing compounds are observed without a significant change in the viscosity of the mixture. The volatile products released fulfill the role of pore-forming. This provides favorable conditions for the formation of relatively similar size and large amount of pores. When they accumulate in sufficient

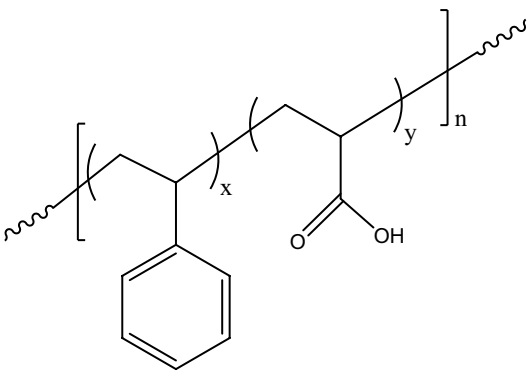

Styrene acrylic copolymer

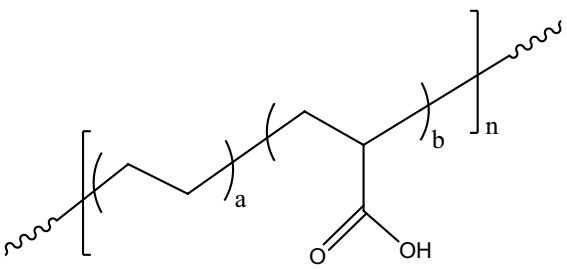

Vinyl acrylic copolymer

Fig. 5 Structural formula of acrylic resins used

Table 2 Mechanical and physical properties of carbon foams

	Shrinkage (vol %)	Density (g/cm^3)	Mechanical strength (MPa)
CF-1:1	69.39 ± 0.02	0.565 ± 0.04	0.837 ± 0.03
CF-1:3	69.82 ± 0.02	0.614 ± 0.04	1.17 ± 0.02
CF-0:5	76.44 ± 0.04	0.723 ± 0.04	1.36 ± 0.04

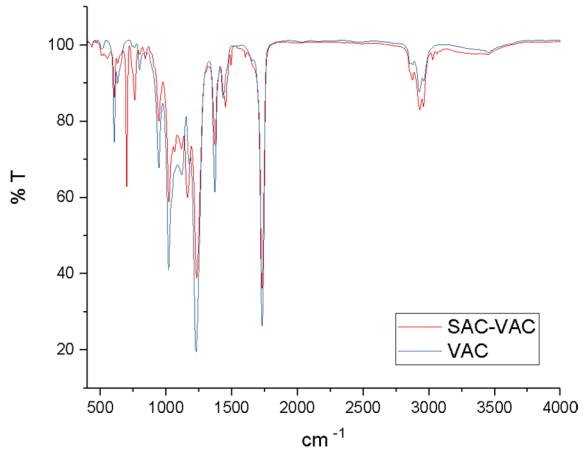

Fig. 6 FT-IR spectrum of cured acrylic resins

amount, synthetic reactions start and cause solid product formation [25].

Polycondensation reactions in the calcination phase of carbon foam production were effective due to the sulfur (4.87%) contained in the structure of the recovered carbon. This sulfur originated from sulfuric acid used in chemical degradation processes of waste tire.

41.88% VM, 5.21% moisture, 6% H and 21.35% O (Table 1), which were in the structure of RC, showed a pore-forming effect in carbon foam production.

The complete removal of resins from the environment during calcination of carbon foams shows that the resulting carbon foams only reveal the characteristics of the natural structure of the RC. In studies conducted, resins such as phenolic, PU, melamine and resorcinol used for the production of carbon foam make coalification by forming the sacrificial template and other additives used helped the pores to be larger. The acrylic resins used in this new method provided the RC powders to adhere and it did not serve as a sacrificial template. However, as in phenolic resins [27], it showed high coalification capacity.

Characterization analysis, mechanical and physical tests were applied to the carbon foams produced as a result of the study of 1:1, 1:3, and 0:5 SAC:VAC ratios. Mechanical and physical test results are given in Table 2. The mechanical strength, shrinkage and density of carbon foams varied depending on the VAC resin used in the process.

The mechanical strength, shrinkage and density of carbon foam produced from sucrose by sintering at 1400 °C was 0.89 MPa, 46.24 vol%, and 0.142 g/cm^3, respectively [49]. The density and mechanical strength of the carbon foam obtained as a result of pyrolysis at 1400 °C by impregnating commercial PU foams with phenolic resin are 0.092 g/cm^3 and 0.23 MPa, respectively [50]. Density and mechanical strength of carbon foams produced from mesophase pitch pellets at 573 K are 0.56 g/cm^3 and 3.31 MPa, respectively [51]. The mechanical strength and density of carbon foams vary depending on the carbon source used and the process applied.

FT-IR analysis is used to determine the chemical composition of carbonaceous materials and functional structures of acrylic resins. FT-IR analysis (Fig. 6) peaks and descriptions (Table 3) determined after curing the SAC–VAC mixture and VAC resins were given.

Curing process in acrylic resin depends on the disappearance of C=CH_2 groups in the monomer. It can be followed by measuring the intensity of specific absorption bands associated with the 812 cm^{-1} C=CH_2 trend or ~1400 cm^{-1} =CH_2 deformation [52]. In the cured VAC given in Table 2, ~1400 cm^{-1} peak was not observed; however, the peak observed at 1450 cm^{-1} of cured SAC:VAC was the C–H peak in the methyl group (–CH_3).

Table 3 FT-IR spectrum interpretations of cured acrylic resins

SAC:VAC (cm^{-1})	VAC (cm^{-1})	Interpretations
2900	2900	Non-asymmetric vibration peak of the aliphatic C–H bond [53]
1730	1730	C=O vibration peak in carboxylic groups [54]
1450	–	Deformation vibration peak of C–H bonds in the methyl group [53]
1370	1380–1370	C–O vibration peak [53]
1220–1214	1220	C–O stress in acrylic aryl ether [55]
1020	1020	C–N stress in the amine group [55]
945–700	945–798	C–H vibration peak [56]
–	605	C–C vibration peak [57]

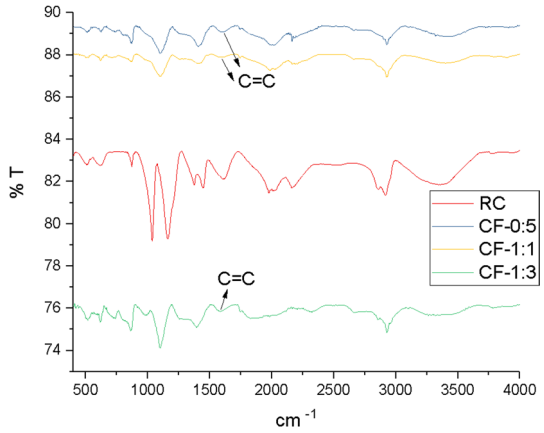

Fig. 7 FT-IR spectrum of carbon foams and RC

The FT-IR spectrum of the recovered carbon and the carbon foams obtained is given in Fig. 7. Peaks of RC are: 3382 cm^{-1} O–H vibration peak [56], ~2900 cm^{-1} non-asymmetric vibration peak of aliphatic C–H bond [53], 2160 cm^{-1} and 2030 cm^{-1} C≡C vibration peak [58], ~1600 cm^{-1} C=O vibration peak in carboxylic groups [54], ~1400 cm^{-1} deformation vibration peak of C–H bonds [53], 1370 cm^{-1} C–O vibration peak [53], 1164 cm^{-1} C=S bond vibration peak [59, 60], 1034 cm^{-1} C–C vibration peak [61], 870 cm^{-1} C–H vibration peak [58], and 630 cm^{-1} and 522 cm^{-1} C–C vibration peak [57].

The peak descriptions of the carbon foams obtained are given in Table 4. The observation of the ~1600 cm^{-1} C=C bond [63] in the skeleton ring of 3D dimensional carbonaceous materials proved that carbon foams were produced.

SEM and TEM views of 1:1 SAC–VAC mixture and VAC resins after curing are given in Fig. 8. Heterogeneous nanoparticles were observed in the cured SAC–VAC mixture structure. Cured VAC structure has a homogeneous surface.

SEM views of the carbon foams obtained are given in Figs. 9, 10, and 11. Porous composite structures were considered as open-celled and closed-celled. At least 90% of the carbon foam cells obtained were open-celled. Due to their high pore ratio, the distribution of pore sizes of carbon foams varies on average between 10 and 500 microns [27]. Pore sizes were determined between 1 and 40 microns for CF-1:1, ~1 micron for CF-1:3, and 100 nm–50 microns for CF-0:5. Average pore size of CF-1:1, CF-1:3, and CF-0:5 were 10.91, 0.215, and 1397.422 µm, respectively. Yu et al. [40] produced carbon foam by carbonizing the coal tar pitch that they produced at 460 at 1600 °C. Collapsed cell structure and small pores were observed on the surface of the carbon foam and many microporous structures were present in its bonds. Since the oxidation resistance of carbon foams was increased with the pentagonal dodecahedron structure, oxidation primarily occurred on the surfaces of these carbon foams. CF-1:3 carbon foam structure was similar to the carbon foam produced by these researchers; however, no micropores were observed in its bonds (Fig. 10). Micropores and nanoparticles were observed in the bonds of CF-0:5 produced using only VAC (Fig. 11). It was established that SAC prevents the formation of micro-porosities in carbon foam production.

The surface area of pyrolyzed carbon foams was approximately 4 m^2/g [65]. The surface areas of the carbon foams obtained were between 40.89 m^2/g and 98.78 m^2/g (Table 5). As the amount of VAC in the carbon foam mixture increased, the surface area and micropores of the carbon foams increased.

Table 4 FT-IR spectrum interpretation of the carbon foams obtained

CF-1:1 (cm^{-1})	CF-1:3 (cm^{-1})	CF-0:5 (cm^{-1})	Interpretation
~3450	~3450	~3450	Water molecule or O–H groups [63]
2935	2935	2935	*Symmetric and asymmetric C–H group [63]
2180	2180	–	Absorbed CO compound [63]
2000	2000	–	C≡N [63]
–	–	1855	$–CH_2$ group [63]
~1600	~1600	~1600	**C = C bond [63]
~1400	~1400	~1400	O–H bans attached to amine group [63]
1100	1100	1100	*** = C–O–C structure [63]
880	880	880	Epoxy (–C–O–C–) group [63]
–	–	740	–COOH group [63]
626	626	626	C–H [27]
~515	~515	~515	Planar ring deformation of the phenyl ring [60]

*Located in CH_2 is the symmetric and asymmetric C–H group and hydrogen is bonded through an sp^3-hybridized carbon

**Aromatic structure found in the skeletal ring (C=C bond)

*** =C–O–C structure of the benzene ring branch in the carboxylic group (–COOH)

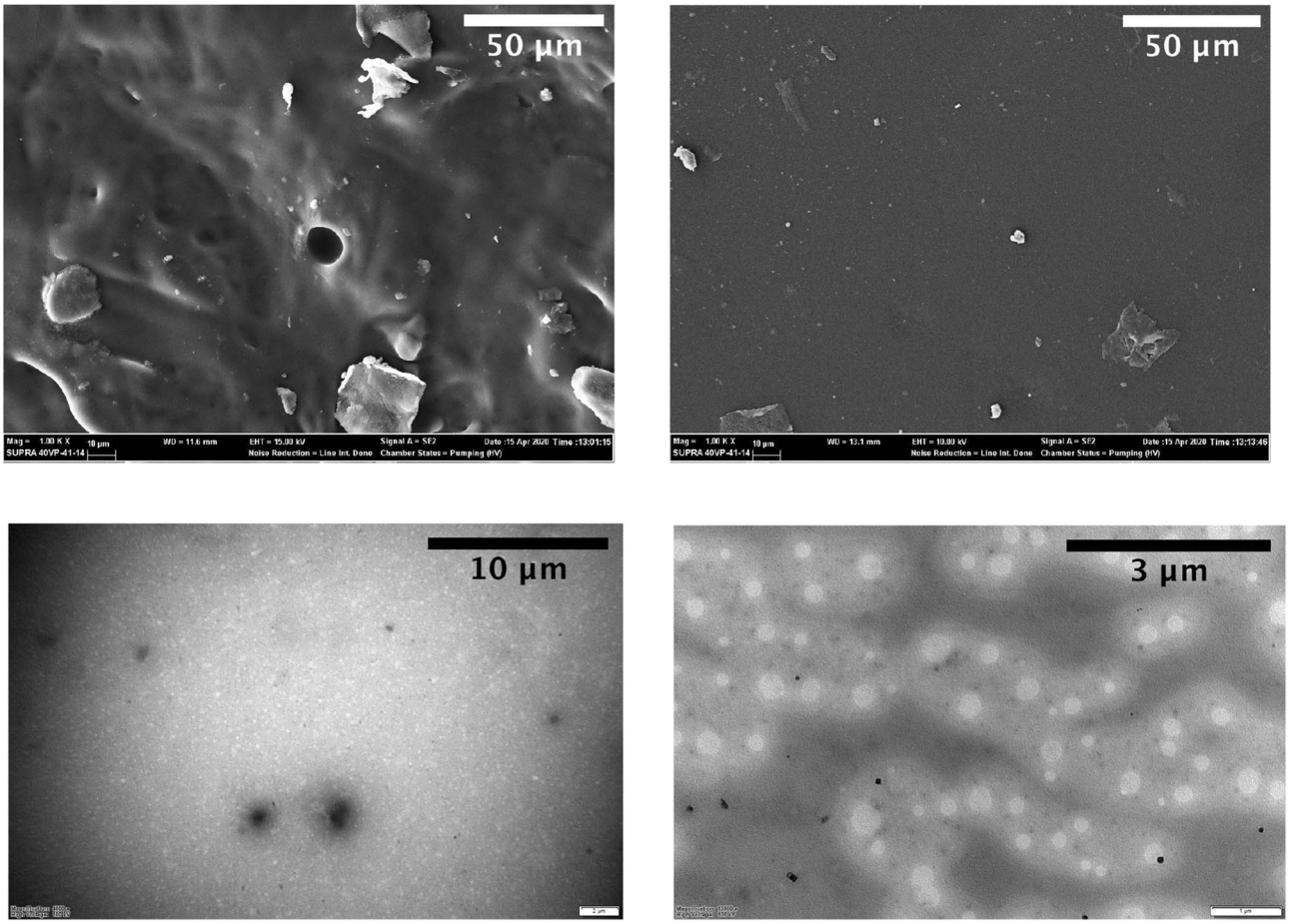

Fig. 8 SEM and TEM views of cured VAC and SAC–VAC (1:1) mix (left-top: VAC (1000×), right-top: SAC–VAC (1000×), left-bottom: TEM for VAC, right-bottom: TEM for SAC–VAC)

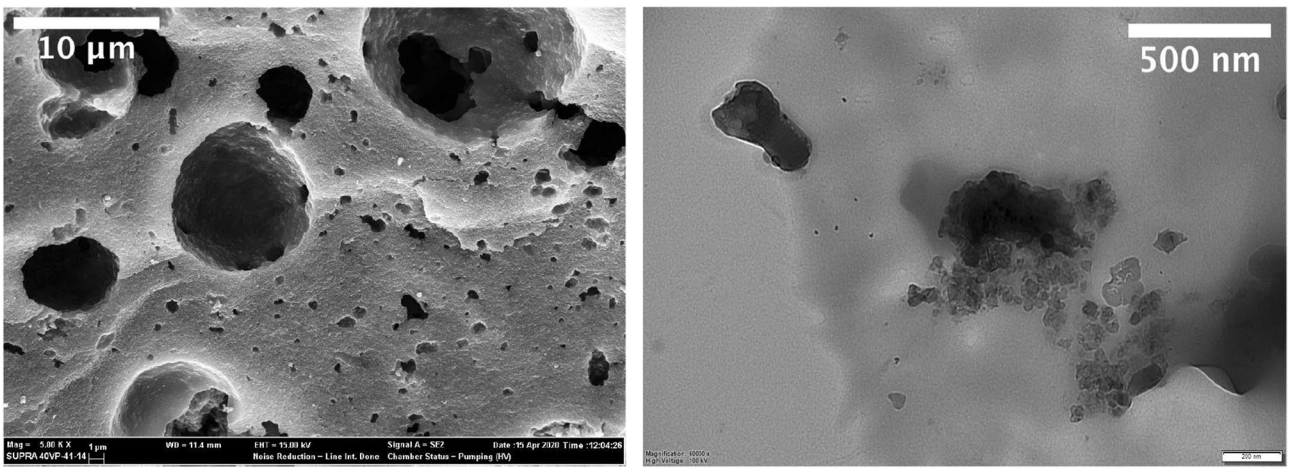

Fig. 9 SEM and TEM views of CF-1: 1 (right: SEM-5000×, left: TEM)

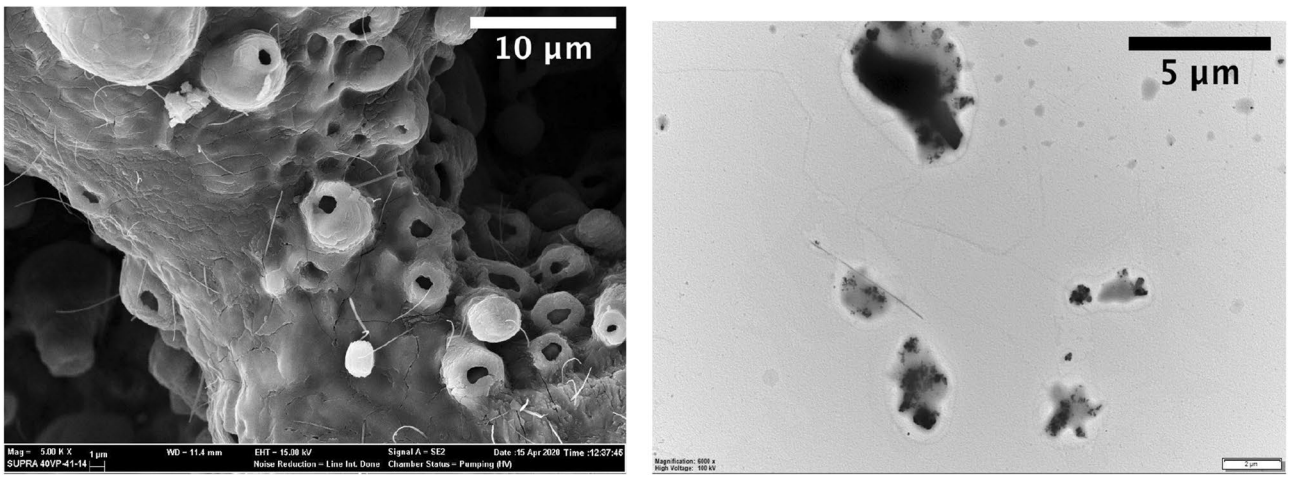

Fig. 10 SEM and TEM views of CF-1: 3 (left: SEM-500×, right: TEM)

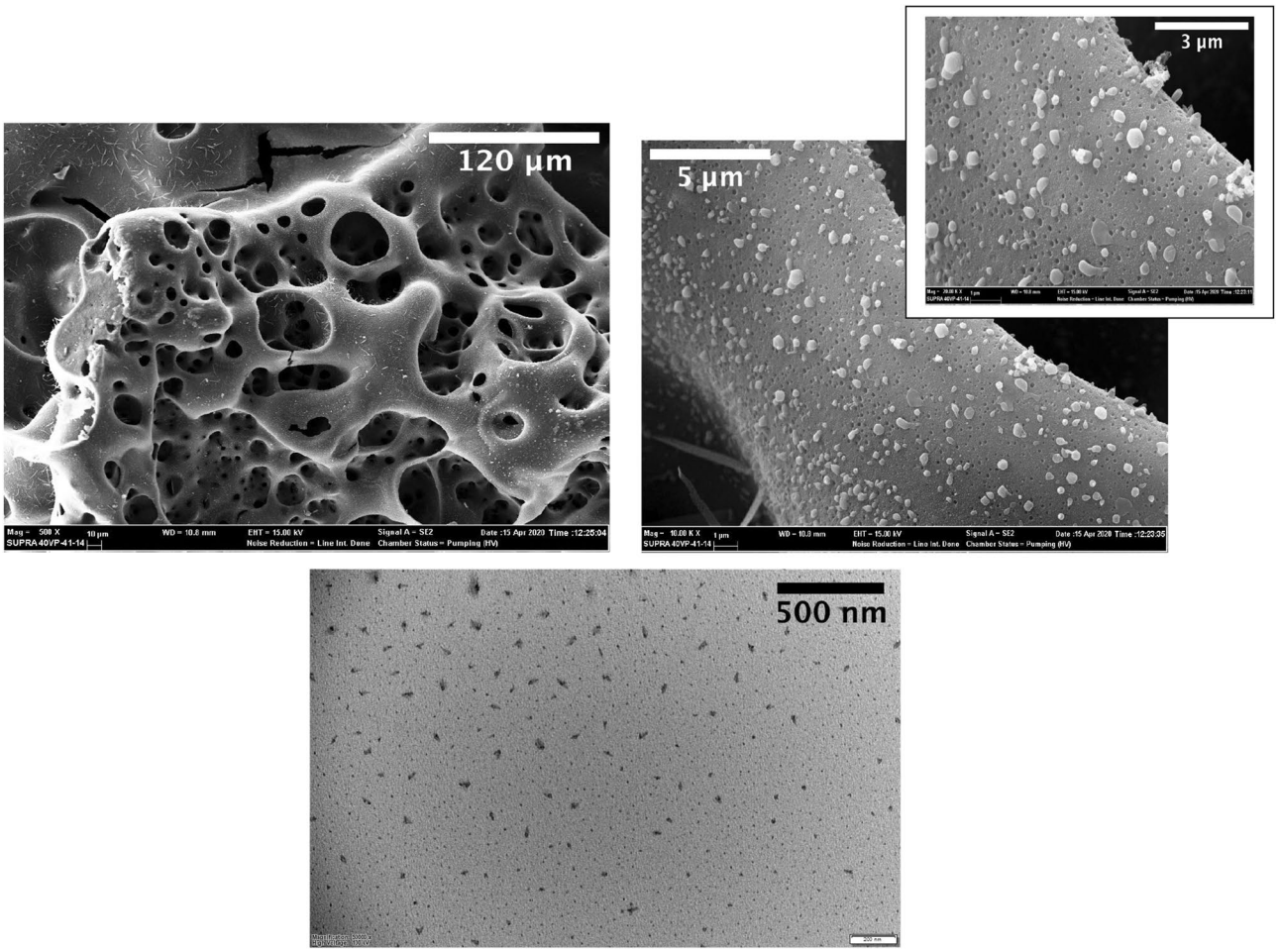

Fig. 11 SEM and TEM views of CF-0:5 (top-left: 500×, top-right: 10,000×, top-right-top: 40.000×, bottom: TEM)

Table 5 Surface area values of RC [17] and carbon foams obtained

	S_{BET} (m^2/g)	S_{ext} (m^2/g)	S_{mic} (m^2/g)	V_t (cm^3/g)	V_{mic} (cm^3/g)	V_{mezo} (cm^3/g)	Nanoparticle size (Å)	Pore width (Å)
RC	35.45	39.7	0	0.125	0	0.125	0.014	414.14
CF-1:1	40.89	12.64	28.25	0.035	0.013	0.022	1467.275	34.42
CF-1:3	72.07	19.37	52.70	0.05	0.024	0.026	832.544	28.31
CF-0:5	98.78	22.68	76.10	0.06	0.035	0.025	607.386	24.11

Conclusion

The aim of the study was to define a new method for the production of carbon foam by curing organic materials with high-volatile content by mixing only with acrylic resins. At the same time, it was revealed that waste tires in the waste class can be used in the production of carbon foam, depending on the use of carbon sources in this new method. RC produced from waste tire was used as a carbon source in the study and using less energy and in a shorter time, and the mixture of RC and water-based acrylic resin was cured in a catalyst-free environment, turning carbon foam which is a valuable product. Different RC quantities (3–4–5 g), SAC:VAC ratios (5:0–3:1–1:1–1:3–0:5), temperature (400–500–600–700–800–900 °C), and time (30–60–120–180–240 min) parameters were determined to be the most suitable working condition at 600 °C and 30 min of 4 g RC. Carbon foams were produced as a result of solution polymerization and polycondensation reactions, respectively. The porosity values of CF-1:1, CF-1:3, CF-0:5 carbon foams were 75.71, 79, and 97%, respectively. The porosity value was 97% due to the micropores and nanoparticles formed in the bonds of CF-0:5 where only VAC was used. As the amount of VAC increased in the carbon foam mixture, the surface area increased.

The complete removal of resins from the environment during calcination of carbon foams shows that the resulting carbon foams only reveal the characteristics of the natural structure of the RC. In studies conducted, resins such as phenolic, PU, melamine and resorcinol used for the production of carbon foam make coalification by forming the sacrificial template and other additives used helped the pores to be larger. The acrylic resins used in this new method provided the RC powders to adhere and it did not serve as a sacrificial template. However, as in phenolic resins, it showed high coalification capacity.

A new method was developed for the production of carbon foam as a result of curing organic substances with high-volatile matter content by mixing only with acrylic resins without using pressure and stabilization steps. Carbon foams were obtained at 600 °C in 30 min. Carbon foams with a temperature effect of <1000 °C or >1000 °C were produced in approximately 2 h during the studies. Therefore, this new described method was more advantageous than the methods given in the literature.

This study not only offers a new technique for producing carbon foam, but also proposes a promising method for producing carbon foam from high organic content wastes for environmental improvement.

Acknowledgements This work was supported by Coordination of Scientific Research Projects (BAP) of the Bilecik Seyh Edebali University (Project No: 2019-01.BSEU.11-02). We would like to thank ASAL Boya Kimya Sanayi Tic.Ltd.Şti. for their free sample support throughout our work.

Declarations

Conflict of interest The authors declare no conflicts of interest.

References

1. Parthasarathy P, Choi HS, Park HC, Hwang JG, Yoo HS, Byeong-Kyu Lee B-K, Upadhyay M (2016) Influence of process conditions on product yield of waste tyre pyrolysis—A review. Korean J Chem Eng 33(8):2268–2286. https://doi.org/10.1007/s11814-016-0126-2
2. Rani S (2014) Recycling of scrap tires. Inter J Mat Sci Appl 3(5):164–167. https://doi.org/10.11648/j.ijmsa.20140305.16
3. Messenger B (2013) https://waste-management-world.com/a/tackling-tire-waste. https://waste-management-world.com/a/tackling-tire-waste. Accessed 21 Aug 2021
4. End-Of-Life Tyre Report (ETRMA) (2015) European Tyre & Rubber Manufacturers' Association, http://www.etrma.org/uploads/Modules/Documentsmanager/elt-report-v9a---final.pdf. Accessed 21 Aug 2021
5. LASDER (2020) Which Tires Are End of Life Tires? http://www.lasder.org.tr/otl-2/otl/. Accessed 21 Aug 2021
6. Li K, Gao XL, Roy AK (2003) Micromechanics model for three-dimensional open-cell foams using a tetrakaidecahedral unit cell and Castigliano's second theorem. Compos Sci Technol 63(12):1769–1781. https://doi.org/10.1016/S0266-3538(03)00117-9
7. Kathomi ML, Maina MW (2013) From waste to product; recycling waste tires to save the environment. http://cae.uonbi.ac.ke. Accessed 21 Aug 2021
8. Karaağaç B, ErcanKalkan M, Deniz V (2017) End of life tyre management: Turkey case. J Mater Cycles Waste Manag 19:577–584. https://doi.org/10.1007/s10163-015-0427-2
9. Control Regulations of End-Of-Life Tires (CRELT), 26357, 25.11.2006

10. End of Life Vehicles Control Regulation (ELVCR), 25679, 23.12.2004
11. EPA (United States Environmental Protection Agency) (2010) ScrapTires: Handbook on Recycling Applications and Management for the U.S. and Mexico, https://nepis.epa.gov/: Accessed 21 Aug 2021
12. Okoro EE, Erivona NO, Sanni SE, Orodu KB, Igwilo KC (2020) Modification of waste tire pyrolytic oil as base fluid for synthetic lube oil blending and production: waste tire utilization approach. J Mater Cycles Waste Manag 22:1258–1269. https://doi.org/10.1007/s10163-020-01018-1
13. Hu Y, Attia M, TsabetMohaddespourMunirFarag EAMTS (2021) Valorization of waste tire by pyrolysis and hydrothermal liquefaction: a mini-review. J Mater Cycles Waste Manag 23:1737–1750. https://doi.org/10.1007/s10163-021-01252-1
14. Osayi JI, Iyuke S, Daramola MO, Osifo P, Van Der Walt IJ, Ogbeide SE (2018) Pyrolytic conversion of used tyres to liquid fuel: characterization and effect of operating conditions. J Mater Cycles Waste Manag 20:1273–1285. https://doi.org/10.1007/s10163-017-0690-5
15. dos Santos RG, Rocha CL, Felipe FLS, Cezario FT, Correia PJ, Rezaei-Gomari S (2020) Tire waste management: an overview from chemical compounding to the pyrolysis-derived fuels. J Mater Cycles Waste Manag 22:628–641. https://doi.org/10.1007/s10163-020-00986-8
16. Burkhanbekov K, Aubakirov Y, Tashmukhambetova Z, Abildin T (2019) Thermal processing of waste tires with heavy oil residue in the presence of Tayzhuzgen zeolite. J Mater Cycles Waste Manag 21:633–641. https://doi.org/10.1007/s10163-018-00825-x
17. Balbay S (2017) Chemical decomposition of waste tires and evaluation of the obtained products. PhD Thesis. Bilecik Seyh Edebali University.
18. Balbay S, Acikgoz C (2019) Devulcanization of waste tyre rubber and solid product obtained from the method. Patent no: 2015/13034
19. Yamashita D, Usui K, Takahashi T, Akutagawa K, Hojo M, Hironaka K, Tagaya H (2020) Chemical recycling of waste tire in high-temperature organic fluid. J Mater Cycles Waste Manag 22:1249–1257. https://doi.org/10.1007/s10163-020-01017-2
20. Balbay S (2020) Effects of recycled carbon-based materials on tyre. J Mater Cycles Waste Manag 22:1768–1779. https://doi.org/10.1007/s10163-020-01064-9
21. Balbay A (2018) Experimental investigation of the effect of nano particle additive to mechanical and buckling properties on composite plate. MSc Thesis. Pamukkale University, Turkey.
22. Balbay A, Yılmaz Y, Balbay Ş (2021) Characterization of E-glass/epoxy modified with recycled rubber particles and multi-walled carbon nanotubes. Eur J Sci Technol (EJOSAT) 23:837–843. https://doi.org/10.31590/ejosat.848319
23. Özüdoğru I, Yigit Avdan Z, Balbay S (2022) A novel carbon-based material recycled from end-of-life tires (ELTs) for separation of organic dyes to understand kinetic and isotherm behavior. Sep Sci Technol 57:2024-2040 https://doi.org/10.1080/01496395.2022.2029489
24. Chithra A, Wilson P, Vijayan S, Rajeev R, Prabhakaran K (2020) Carbon foams with low thermal conductivity and high EMI shielding effectiveness from sawdust. Ind Crops Prod 145:112076. https://doi.org/10.1016/j.indcrop.2019.112076
25. Stoycheva I, Tsyntsarski B, Vasileva M, Petrova B, Georgiev G, Budinova T, Szeluga U, Pusz S, Kosateva A, Petrov N (2020) New method for synthesis of carbon foam on the base of mixture of coal tar pitch and furfural without using pressure and stabilization treatment. Diam Relat Mater 109:108066. https://doi.org/10.1016/j.diamond.2020.108066
26. Wang T, Zhu C, Song L, Du P, Yang Y, Xiong J (2020) A facile controllable preparation of highly porous carbon foam and its application in photocatalysis. Mater Res Bull 122:110697. https://doi.org/10.1016/j.materresbull.2019.110697
27. Rao GS, Nabipour H, Zhang P, Wang X, Xing W, Song L, Hu Y (2020) Lightweight, hydrophobic and recyclable carbon foam derived from lignin–resorcinol–glyoxal resin for oil and solvent spill capture. J Mater Res Technol 9(3):4655–4664. https://doi.org/10.1016/j.jmrt.2020.02.092
28. Cao M, Feng Y, Tian R, Chen Q, Chen J, Jia M, Yao J (2020) Free-standing porous carbon foam as the ultralight and flexible supercapacitor electrode. Carbon 161:224–230. https://doi.org/10.1016/j.carbon.2020.01.093
29. Chen Y, Qiu X, Fan LZ (2020) Nitrogen-rich hierarchically porous carbon foams as high-performance electrodes for lithium-based dual-ion capacitor. J Energy Chem 48:187–194. https://doi.org/10.1016/j.jechem.2020.01.024
30. Liu H, Xu Y, Tang C, Li Y, Chopra N (2019) SiO_2 aerogel-embedded carbon foam composite with Co-enhanced thermal insulation and mechanical properties. Ceram Int 45(17):23393–23398. https://doi.org/10.1016/j.ceramint.2019.08.041
31. Deng X, Bai X, Cai Z, Huang M, Chen X, Huang B, Chen Y (2020) Renewable carbon foam/δ-MnO2 composites with well-defined hierarchical microstructure as supercapacitor electrodes. J Mater Res Technol 9(4):8544–8555. https://doi.org/10.1016/j.jmrt.2020.05.130
32. Qiu R, Fei R, Zhang T, Liu X, Jin J, Fan H, Wang R, He B, Gong Y, Wang H (2020) Biomass-derived, 3D interconnected N-doped carbon foam as a host matrix for Li/Na/K-selenium batteries. Electrochim Acta 356:136832. https://doi.org/10.1016/j.electacta.2020.136832
33. Pushkar P, Mungra AK (2020) Exploring the use of 3 dimensional low-cost sugar-urea carbon foam electrode in the benthic microbial fuel cell. Renew Energy 147:2032–2042. https://doi.org/10.1016/j.renene.2019.09.142
34. Ai D, Hongqıang W, Chen Z, Bın Z (2019) Ultra-black carbon aerogel foam compound and preparation method thereof. Patent No. CN 110451478.
35. Aihua C, Yongfei L, Bosheng Z, Xin H (2019) Activated carbon foam prepared from activated carbon absorbing waste gas in polyurethane foaming process and preparation method thereof, Patent No. CN 110407999A.
36. Ningjing S (2017) Flexible self-supporting SnS/carbon foam composite material and preparation method and application thereof, Patent No. CN107895786A.
37. Canhui L, Jiangqi Z, Wei Z, Qingye L (2018) Preparation method of multifunctional carbon foam, Patent No. CN109437147A.
38. Zhou X, Jia Z, Feng A, Wang X, Liu J, Zhang M, Cao H, Wu G (2019) Synthesis of fish skin-derived 3D carbon foams with broadened bandwidth and excellent electromagnetic wave absorption performance. Carbon 152:827–836. https://doi.org/10.1016/j.carbon.2019.06.080
39. Inagaki M, Qiu J, Guo Q (2015) Carbon foam: preparation and application. Carbon 87:128–152. https://doi.org/10.1016/j.carbon.2015.02.021
40. Yu M, Li C, Ao X, Chen Q (2019) Fabrication of coal tar pitch–derived reticulated carbon foam as oxidation-resistant thermal insulation. J Anal Appl Pyrolysis 141:104643. https://doi.org/10.1016/j.jaap.2019.104643
41. Liu X, Wang S, Sun C, Liu H, Stevens L, Dwomoh PK, Snape C (2020) Synthesis of functionalized 3D microporous carbon foams for selective CO2capture. Chem Eng J 402:125459. https://doi.org/10.1016/j.cej.2020.125459
42. Zimmermann MVG, Perondi D, Lazzari LK, Godinho M, Zattera AJ (2020) Carbon foam production by biomass pyrolysis. J Porous Mater. https://doi.org/10.1007/s10934-020-00888-y

43. Eksilioglu A (2004) Investigation of the effects of temperature, solvent and additional carbon materials on the properties of mesophase pitch-based carbon foam. Master Thesis. İstanbul Technical University
44. Tan J, Li W, Ma C, Wu Q, Xu Z, Liu S (2018) Synthesis of honeycomb-like carbon foam from larch sawdust as efficient absorbents for oil spills cleanup and recovery. Materials 11:1106. https://doi.org/10.3390/ma11071106
45. De S, Acharya S, Sahoo S, Chandra Nayak G (2020) Present status of biomass-derived carbon-based composites for supercapacitor application. Nanostructured, Functional, and Flexible Materials for Energy Conversion and Storage Systems. Chapter 12. 373–415. https://doi.org/10.1016/b978-0-12-819552-9.00012-9
46. OL Li T Ishizaki 2018 Development, challenges, and prospects of carbon-based electrode for lithium-air batteries Emerg Mater Energy Convers Storage 115–152 https://doi.org/10.1016/B978-0-12-813794-9.00004-1
47. Nagel B, Pusz S, Trzebicka B (2014) Review: tailoring the properties of macroporous carbon foams. J Mater Sci 49(1):1–17. https://doi.org/10.1007/s10853-013-7678-x
48. Aygun M (2004) Oil Based Polymer Production by Emulsion Polymerization Method. Master Thesis. Istanbul Technical University
49. Prabhakaran K, Singh PK, Gokhale NM, Sharma SC (2007) Processing of sucrose to low density carbon foams. J Mater Sci 42:3894–3900. https://doi.org/10.1007/s10853-006-0481-1
50. Manocha SM, Patel K, Manocha LM (2010) Development of carbon foam from phenolic resin via template route. Indian J Eng Mater Sci 17:338–342
51. Eksilioglu A, Gencay N, Yardim MF, Ekinci E (2006) Mesophase AR pitch derived carbon foam: effect of temperature, pressure and pressure release time. J Mater Sci 41(10):2743–2748. https://doi.org/10.1007/s10853-006-7079-5
52. Lozano E, Spragg DR (2011) Introduction FT-IR Spectroscopy Analysis of UV-Curable Resins by FT-IR. www.perkinelmer.com. Accessed 21 Aug 2021
53. Wu B, Zhou MH (2009) Recycling of waste tire rubber into oil absorbent. Waste Manag 29(1):355–359. https://doi.org/10.1016/j.wasman.2008.03.002
54. Zhao Y, Zhang Y, Zhang H, Wang Q, Guo Y (2015) Structural characterization of carbonized briquette obtained from anthracite powder. J Anal Appl Pyrolysis 112:290–297. https://doi.org/10.1016/j.jaap.2015.01.009
55. Sigma Aldrich (2020) IR Spectrum Table by Frequency Range, https://www.sigmaaldrich.com/technical-documents/articles/biology/ir-spectrum-table.html. Accessed 21 Aug 2021
56. Li W, Zhu YM, Wang G, Jiang B (2016) Characterization of coalification jumps during high rank coal chemical structure evolution. Fuel 185:298–304. https://doi.org/10.1016/j.fuel.2016.07.121
57. Tiryaki B (2013) Activated carbon production from cellulose, hemicellulose and lignin. Master Thesis. Ankara University
58. OChemOnline (2011) Infrared spectroscopy absorption table http://www.ochemonline.com/Infrared_spectroscopy_absorption_table. Accessed 21 Aug 2021
59. Borah D (2005) Desulphurization of organic sulphur from coal by electron transfer process with Co 2+ ion. Fuel Process Technol 86(5):509–522. https://doi.org/10.1016/j.fuproc.2004.04.004
60. Trivedi MK, Patil S, Shettigar H, Bairwa K, Jana S (2015) Effect of biofield treatment on spectral properties of paracetamol and piroxicam. Chem Sci J 6:98. https://doi.org/10.4172/2150-3494.100098
61. Genceli FE (2000) Evaluation of apricot kernel as a raw material for carbon material production: obtaining tar and pitch. Master Thesis. İstanbul Technical University
62. Sarici Ozdemir C (2008) Çeşitli polimerik temelli atıklardan yüksek yüzey alanlı aktif karbon eldesi, karakterizasyonu ve uygulama alanları. PhD Thesis. İnönü University
63. Ţucureanu V, Matei A, Avram AM (2016) FTIR spectroscopy for carbon family study. Crit Rev Anal Chem 46(6):502–520. https://doi.org/10.1080/10408347.2016.1157013
64. Yang C, Wöll C (2017) IR spectroscopy applied to metal oxide surfaces: adsorbate vibrations and beyond. Adv Phys X. 2(2):373–408. https://doi.org/10.1080/23746149.2017.1296372
65. Pham TN (2016) Three-dimensional structured carbon foam: Synthesis and Applications, Umeå University. Department of Chemistry. Doctoral thesis